Causality of the damages in high power rotating system elements: Experimental testing and modeling

V. Barzdaitis[1], M. Bogdevičius[2]

[1]*Kaunas University of Technology, Engineering Mechanics Department, Lithuania*
vytautas.barzdaitis@ktu.lt,
[2]*Vilnius Technical University, Department of Transport Technological Equipment, Lithuania*
marius@vtu.lt

Abstract

This article concerns dynamics of high power rotating system with toothed wheel coupling. The elastic contacts located between plates and between plate's packets and semi couplings teeth. Friction between plates inside packet and teeth generates fretting corrosion phenomenon and damages plates. Theoretical modeling and simulation of rotating system was provided by a finite element method**.** Complex model involved rotating system, hydrodynamic bearings and coupling. The dynamics of semi couplings and plates have been simulated end experimentally monitored. The experimental testing of rotating system was provided by stationary machine condition monitoring and diagnostic system. High frequency absolute vibration acceleration, however, make it possible to determine the technical condition of toothed wheel coupling, which is difficult to determine by applying the shafts vibration.

Keywords: : dynamics, modeling, rotating system, bearings, diagnostic.

Introduction

The reliability and efficiency is main problem that supports renovations of the high power generating machines. Experimental testing in situ with modeling and simulation of dynamics of these rotating systems supports failure preventive methods design and installation.

In this article the dynamics of two steam turbines rotating systems with flexible coupling is presented. The high pressure cylinder rotor (1, HPR) medium and low pressure cylinder rotor (2, MLPR) is joined with nonlinear flexible coupling (3, NFC). The rotating system is shown in Figure 1. Two semi couplings with 80 teeth each are connected by plate's packets. Each packet contains three plates.

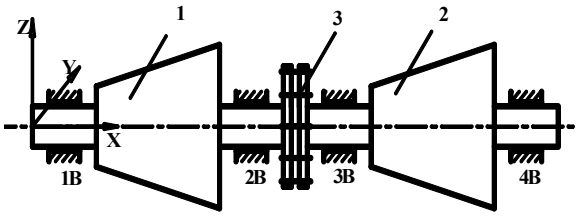

Fig. 1. **Rotor and bearing system: 1 – high pressure cylinder rotor (HPR); 2 – medium and low pressure cylinder rotor (MLPR); 3 – nonlinear flexible coupling (NFC); kB – journal bearings, k=1,..,4**

Transferring the torque the rotating system vibrates mainly by the dynamic forces acting from unbalance, misalignment and from NFC elements motion. The dynamics of NFC depends on each plate motion in the packet, plate's pockets motion and relative motion between each semi couplings. The high rotating velocity generates large inertia forces acting on plates. The plates radial motions are limited by the cylinder that is fixed on the HPR semi coupling.

Plates motions in the coupling is complicated, initiated metallic contact between plates and plate's inside the packets and with teeth. Because of friction between plates inside packet and plate's packets and teeth the fretting corrosion phenomenon take place that additionally damages plates as shown in Fig. 2. Fretting corrosion is caused by a relative motion of mated contact surfaces and results as contact failures. The evaluation of technical condition of rotating system with NFC through motion of plate's packets and vibration of semi couplings is the task of this article.

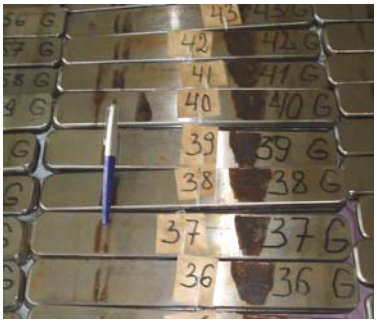

Fig. 2. **General view of damaged plates**

Experimental testing in situ

The proximity probes measures relative displacements of shafts in the bearings and vibration displacements of the shafts relative to bearings but not the motion of coupling or its elements. Modeling and simulation of rotating system with NFC was provided using experimental data.

For monitoring vibration of rotating system the absolute vibration of the bearings and relative vibration displacements of the shafts were used [3-5].

With a stationary installed monitoring system the peak-to-peak shafts relative displacements $S_{(p-p)}$, radial gaps ΔX and ΔY, unbalance vectors, ect., have been measured and the maximum values of vibration

displacement S_{max} were calculated referring to ISO 7919. One of the basic differences in the operation of driving and driven semi couplings lies in the bearings design - the 2nd bearing is radial while the 3rd one is radial-axial. The radial-axial bearing significantly changes the orbit of the motion of the 3rd bearing shaft together with driven semi coupling, Fig. 3a,b. The squared elliptical area of the 2nd bearing orbit is greater compared with the non-elliptical orbit of the 3rd bearing shaft. When changing the load the same ratio of the limited orbits areas remains as stable but different shapes of the orbits.

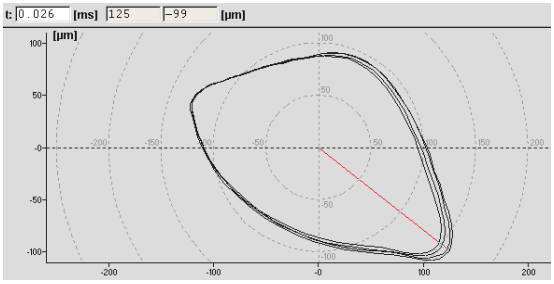

Fig. 3a. **HPR 2nd bearing shaft kinetic orbit s_{max2}=158 µm at 51 MW power**

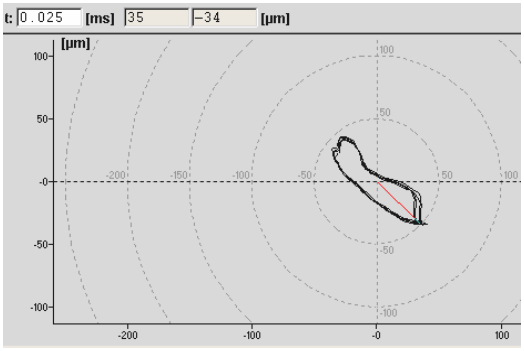

Fig 3b. **MLPR 3rd bearing shaft kinetic orbit s_{max3}=55 µm at 51 MW power**

This causes the changes of the eccentricity ratios of the 2nd and 3rd bearings, affects alignment of HPR and MLPR and changes design axial positions of both semi couplings. Eccentricity ratio of 1st and 2nd bearings also depends on instabilities of the steam control system of the HPR and MLPR.

The TWC generates high frequency vibration approaching 4000 Hz and 2X harmonic (80 teeth with plate's packets at 50 Hz rotation velocity). The relative vibration displacement of 2nd and 3rd bearings either partially evaluated or entirely do not represent the high frequency vibration excited by the NFC. The frequency difference and vibration acceleration intensity is the indicator that plates and plate's packets having been unequally loaded or damaged.

These changes are caused not only due to irregularities of the teeth pitches, deviations of the teeth geometric shape, mechanical and temperature unbalance, etc., but mainly caused by HPR semi coupling radial vibration displacements, caused by unbalance and misalignment of HPR semi coupling and HPR relative to MLPR, Fig. 4.

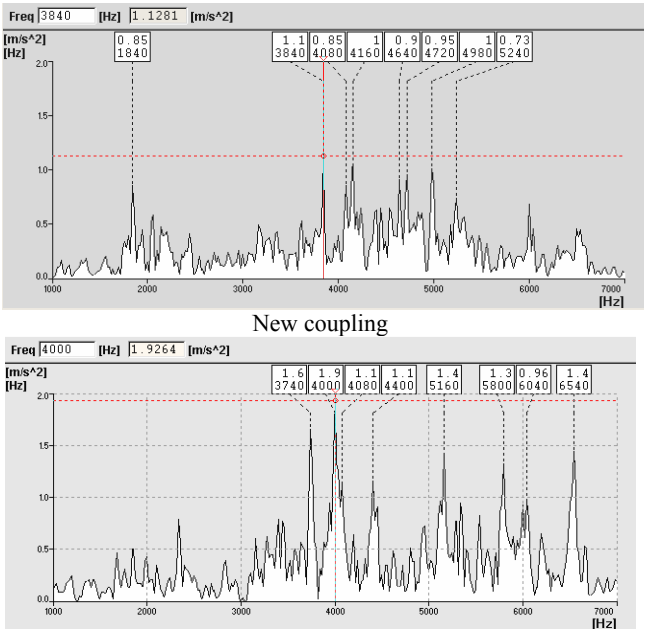

Fig. 4. **The two spectra of vertical vibration acceleration of the HPR 2nd bearing at 54 MW load, after one year in continuous run of machine**

The TWC generates dynamic forces that damage the plates.As shown in Fig. 4, damaged coupling generates higher intensity vibration acceleration in comparison with new coupling. The vibration excited by the coupling plate's packets fall into the high frequency zone and is characterized by absolute vibration accelerations of the 2nd and 3rd bearings. The design and operation of TWC is similar as gearing. The high frequency vibration acceleration spectra of 2nd and 3rd bearing look analogous. The typical spectrum as the 2nd bearing acceleration is shown in Fig. 3. The prevailing high frequency ~4000 Hz vibration acceleration amplitude.

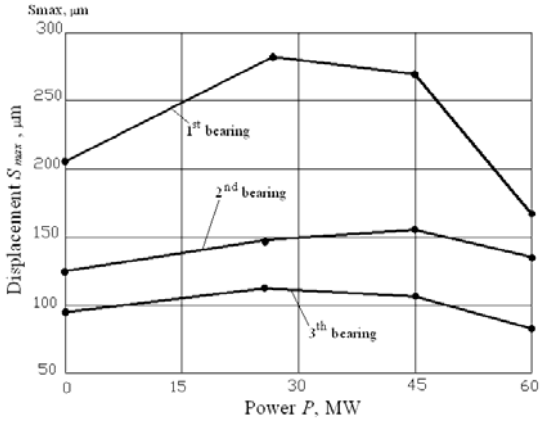

Fig. 5**. Maximum values of vibration displacement S_{max} of the 1st ,2nd and 3rd bearings shafts under varying load**

The valuable changes in average shafts centerline positions strongly depends on loading and indirectly indicate that driving and driven semi couplings possess changes in alignment that generates dynamic forces acting on plates and plates packets.

According absolute vibration intensity v_{rms} values machine can run safely in long term continuous operation mode. But 1st and 2nd bearings shafts relative vibration

maximum values of displacements ($S_{(p\text{-}p)max}$=2 S_{max}, Fig.3) are to high for safe long-term continuous operation because reached vibration severity zone D ($S_{(p\text{-}p)max}$>260 μm, ISO 7919-2:2001). The shafts relative vibration displacement maximum values S_{max} should be considered in condition monitoring of machine.

Models of rotating system

The rotating system shown in Fig. 1 consists of two rotors supported by oil-film bearings with NFC. The following general assumptions have been made: the material of rotors and a coupling are elastic; shear forces are taken into account; the deflection of the rotor is produced by the displacement of points of the centre line; the axial motion of the rotors is neglected; the semi-couplings are treated as rigid.

The rotor dynamics is simulated by the finite element method when the finite element consists of two nodes and five degrees of freedom (DOF) at each node. The first and the second DOF are displacements along y and z axes and the last three DOF are angles around X, Y and Z axes.

The equations of motion of the rotor finite element are derived by applying Lagrange equation of the second order and can be written as follows:

$$[M(q)]\{\ddot{q}\}+([C]+[G])\{\dot{q}\}+[K]\{q\}=\{F(q,\dot{q})\} \qquad (1)$$

where $[M(q)]$,$[C]$, $[G]$ and $[K]$ are mass, damping, gyroscopic and stiffness matrices of the finite element, respectively; $\{F(q,\dot{q})\}$ is the load vector of the finite element.

Under the assumption of small displacements of the journal centre, the fluid-film force components in the horizontal and vertical directions, F_y and F_z, are as follows turns out to be

$$\{F_b\}=\begin{bmatrix} c_{yy} & c_{yz} \\ c_{zy} & czz \end{bmatrix}\begin{Bmatrix} \dot{v} \\ \dot{w} \end{Bmatrix}+\begin{bmatrix} k_{yy} & k_{yz} \\ k_{zy} & k_{zz} \end{bmatrix}\begin{Bmatrix} v \\ w \end{Bmatrix}=$$

$$[C_b]\begin{Bmatrix} \dot{v} \\ \dot{w} \end{Bmatrix}+[K_b]\begin{Bmatrix} v \\ w \end{Bmatrix}, \quad (2)$$

where k_{ij} and the c_{ij} $(i,j)=(y,z)$ are stiffness and damping coefficients, respectively (Fig. 6).

The equations of motion of the coupling can be presented by the matrix equation

$$\begin{bmatrix} [M_{c1}] & [0] \\ [0] & [M_{c2}] \end{bmatrix}\begin{Bmatrix} \ddot{q}_{c1} \\ \ddot{q}_{c2} \end{Bmatrix}+\begin{bmatrix} [G_{c1}] & [0] \\ [0] & [G_{c2}] \end{bmatrix}\begin{Bmatrix} \dot{q}_{c1} \\ \dot{q}_{c2} \end{Bmatrix}=$$

$$\begin{Bmatrix} F_{cg1} \\ F_{cg2} \end{Bmatrix}+\{F_c\}+\{F_w\},$$

or

$$[M_{coupl}]\{\ddot{q}_{coupl}\}+[G_{coupl}]\{\dot{q}_{coupl}\}=\{F_{coupl}\}, \qquad (3)$$

The mass $[M_{ci}]$ and gyroscopic $[G_{ci}]$ matrices and load vectors $\{F_{cgi}\}$of semi coupling are obtained by using second order Lagrange's equation. $\{F_w\}$ is load vector of weight force.

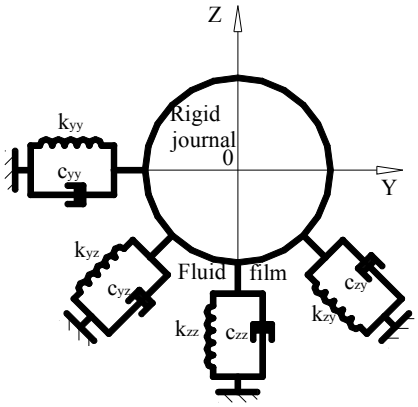

Fig. 6. **Fluid-film model**

Results and discussions

Two steel rotors with toothed wheel coupling rotating at 3000 rpm and supported at the four hydrodynamics bearings are considered (Fig. 1). The values of stiffness coefficients of the bearings are as follows:

$k_{yy}=100.0\times10^6\ \ N/m$,

$k_{yz}=50.0\times10^6\ \ N/m$,

$k_{zy}=-20.0\times10^6\ \ N/m$,

$k_{zz}=300.0\times10^6\ \ N/m$,

$c_{yy}=c_{zz}=50.0\times10^3\ \ Ns/m$,

$c_{yy}=c_{zz}=0$.

The density and elastic modulus of the rotors and coupling material are $\rho=7850\ \ kg/m^3$, $E=210\times10^9\ \ N/m^2$, respectively. Each rotor is divided into 22 finite elements. The number of notches is equal to $NZ=80$, the gap between the plate packet and semi-coupling is design $\delta=90\times10^{-6}\ \ m$. The coefficients of stiffness and damping of plate packet are $k_y=7.47\times10^9\ \ N/m$, $k_z=1.050\times10^9\ \ N/m$, $c_y=5.0\times10^3\ \ Ns/m$, respectively, and the friction coefficient between the plate and semi-coupling is equal to $f=0.10$. The radii of the coupling are $R_0=0.424\ \ m$, $R_1=R_2=0.374\ \ m$. The geometrical parameters of the coupling are $a_1=a_2=0.035\ \ m$, $b=15.180\ \ \times10^{-3}\ \ m$. The mass, polar and transverse moments of the semi-coupling are $m_1=m_2=241\ \ kg$ $J_{cp}=2.15\times10^{-3}\ \ m^4$, $J_{cd}=1.075\times10^{-3}\ \ m^4$. The journal diameter is equal to

0.300 m with the length of 0.300 m; bearing radial clearance "lemon type" is $\sim 350 \times 10^{-6}$ m.

The simulation results are shown in Fig. 7 and Fig. 8 as vibration acceleration spectra in vertical and horizontal directions.

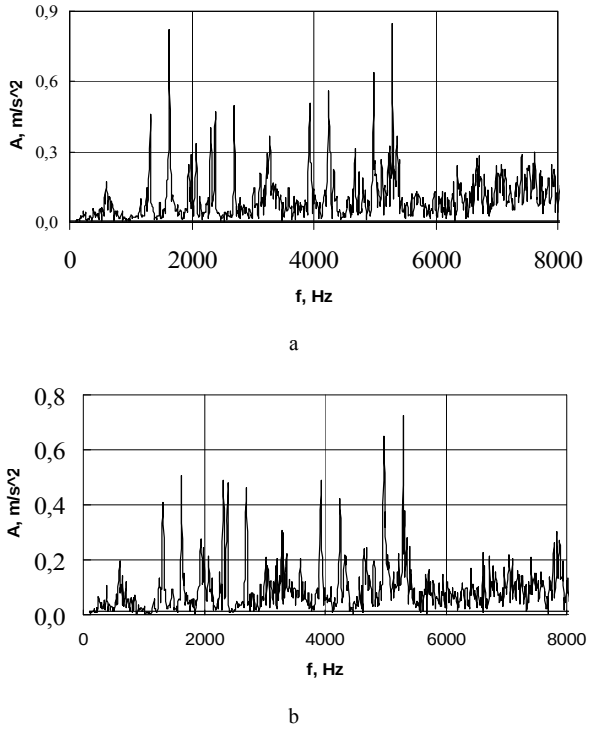

Fig. 7. **The spectra of absolute vibration accelerations of the HPR semi-coupling when the load is 40 MW: a – horizontal direction, b – vertical direction**

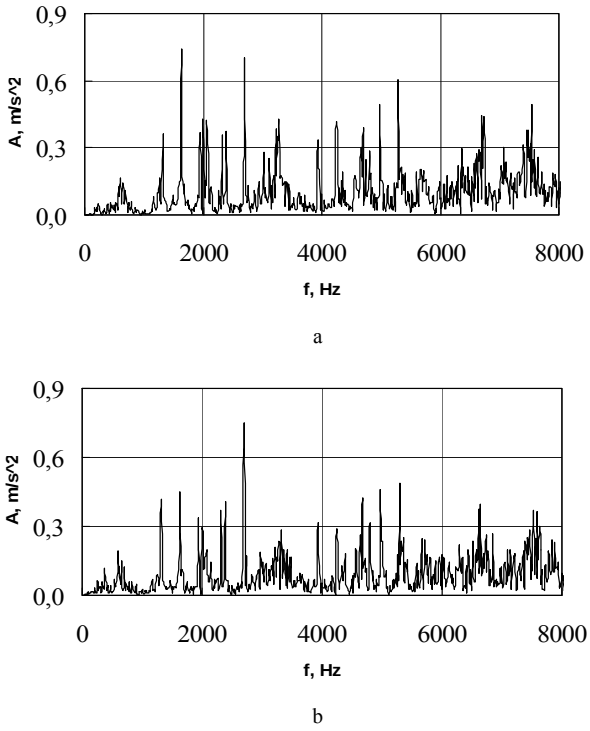

Fig. 8. **The spectra of absolute vibration accelerations of the LMPR semi-coupling when the load is 40 MW: a – horizontal direction, b – vertical direction**

In comparison with experimental data in Fig. 3 the simulation results have the same shape and indicates the acceptance of physical modeling results.

More calculations made on dynamics of plates in the coupling. The vibration displacements results are showed in Fig. 9 and Fig. 10, as vibration displacement values of plate in XYZ coordinate system. The vibration displacements S(p-p) values received in simulation are valuable in diagnostics, because to measurement of vibration displacements of the semi couplings is very complicated and expensive.

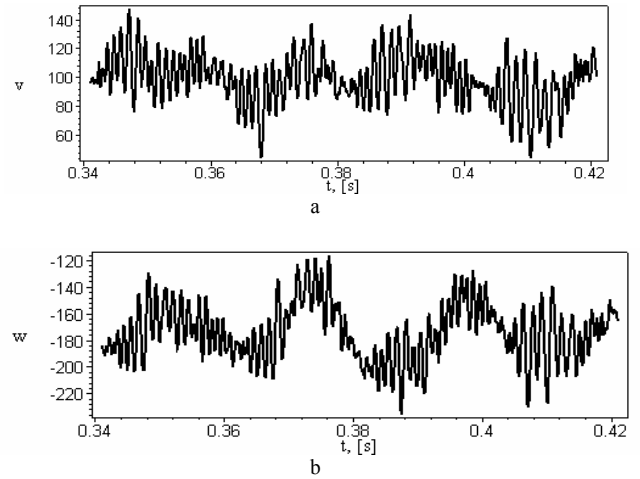

Fig. 9. **Vibration displacements of HPR semi coupling during full four rotations in the XYZ coordinate system at 40 MW power load: a – vertical direction; b – horizontal direction, v, w $[10^{-6} m]$**

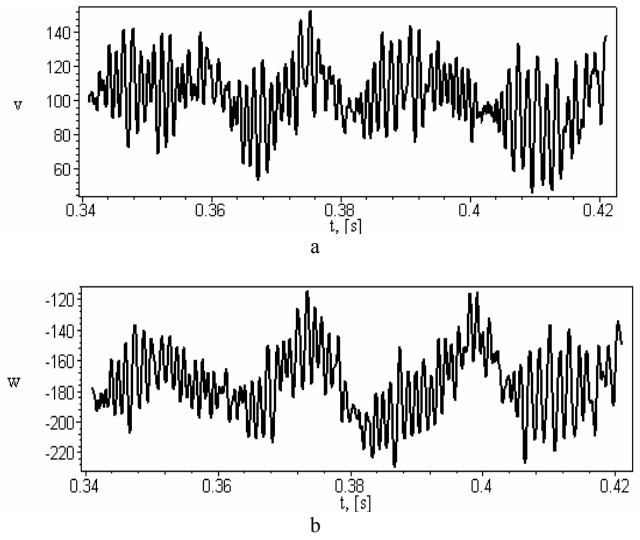

Fig. 10. **Vibration displacements of MLPR semi coupling during full four rotations in the XYZ coordinate system at 40 MW power load: a – vertical direction; b – horizontal direction, v, w $[10^{-6} m]$.**

Conclusions

Rotors and the bearing system with nonlinear flexible coupling were modeled and simulated through the use of the finite element method. Both the gyroscopic effect due

to rotor spin motion and dynamic properties of the oil-film bearings were taken into account in the model.

The dynamic model of rotating system estimates the dynamics of semi-couplings and plate packets. The simulation of the dynamic model of toothed wheel coupling and the analysis of the vibration displacements of semi-couplings and plate packets determine the conditions of the fretting corrosion.

The simulation results provide the basic knowledge in the estimation of the dynamics of semi-couplings and plates because experimental measurement of these parameters is complicated in comparison with shafts' vibration displacements inside the journal bearings.

Absolute vibration acceleration of high frequencies is the main parameter taken into account in practice when evaluating the technical condition and reliability of the whole rotating system.

References

1. **Barzdaitis V., Bogdevičius M., Gečys S.** Vibration problems of high power air blower machine. The 2-nd Internation Symposium on Stability Control of Rotating Machinery (ISCORMA-2). Gdansk. 4 - 8 August 2003. P. 606 – 616.
2. ISO 10816-2 (1996) Mechanical vibration. – evaluation of machine vibration by measurements on non-rotating parts. Part 2. Large – based steam turbine generator sets in excess of 50 MW, 8 p.; P.20. ISO 7919-2 (2001) Mechanical vibration – evaluation of machine vibration by measurements on rotating shafts. Part 2: Land – based steam turbines and generators in excess of 50 MW with normal operating speeds of 1500 r/min, 1800 r/min, 3000 r/min and 3600 r/min. P.20.
3. **Barzdaitis V., Barzdaitis V.V., Didžiokas R., Pocius Z.** Inconsistence of absolute and relative vibration in rotors diagnostics. Mechanika. ISSN 1392-1207. Kaunas: Technologija. 2003. Nr.3(41). P.48-54.
4. **Barzdaitis V., Činikas G.** Monitoring and diagnostics of rotor machines. Monograph. Kaunas: Technologija. 1998. P. 364.
5. **Aladjev V., Bogdevičius M., Prentkovskis O.** New software for mathematical package Maple of releases 6, 7 and 8. Monograph. Vilnius: Technika. 2002. P.404.

V. Barzdaitis, M. Bogdevičius

Didelės galios rotorinės sistemos elementų sužalojimo priežastys: eksperimentiniai tyrimai ir modeliavimas

Reziumė

Nagrinėjama didelės galios rotorinė sistema, kurioje rotoriai sujungti sudėtingos konstrukcijos mova. Movoje yra aštuoniasdešimt išdrožų su komplektu plokštelių. Perduodant sukimo momentą, tarp pusmovių ir plokštelių atsiranda kintamas kontaktas ir veikia kintamos trinties jėgos, o besitrinančiuose kūnų paviršiuose - fretingo korozija. Atlikti rotorinės sistemos eksperimentiniai ir teoriniai tyrimai. Rotorinės sistemos dinaminiai procesai išnagrinėti baigtinių elementų metodu. Rotorinės sistemos eksperimentiniai tyrimai atlikti naudojant stacionarią monitoringo ir diagnostikos sistemą. Gauti rotoriaus absoliučiųjų pagreičių spektrai. Sunku išmatuoti movos ir plokštelių virpesius.

Pateikta spaudai 05 06 2006